Progress in Materials Science xxx (xxxx) xxx

Contents lists available at ScienceDirect

Progress in Materials Science

journal homepage: www.elsevier.com/locate/pmatsci

Construction of equilibrium phase diagrams: Some errors to be avoided

David E. Laughlin [a,b,*], T.B. Massalski [a]

[a] Department of Materials Science and Engineering, Carnegie Mellon University, United States
[b] ALCOA Professor of Physical Metallurgy, Carnegie Mellon University, United States

ARTICLE INFO

Keywords:
Construction errors of phase diagrams
Equilibrium phase diagram
First order transformations
Higher order transformations
Improbable thermodynamic constructions
Phase equilibrium
Third Law of Thermodynamics

ABSTRACT

Guided by the laws of thermodynamics, phase diagrams can be constructed to display First Order phase transformations (Gibbsian), as well as Higher Order phase transitions (non-Gibbsian). We discuss one and two-component alloy systems in this paper. The principles of the construction of phase diagrams are presented and some of the documented construction errors mentioned in the literature that can arise in phase diagram construction are noted and discussed. We go on to discuss what have been termed "probable errors" of construction. These are constructions which could only arise from the application of highly unlikely solution thermodynamic expressions. We then discuss the application of the Third Law of Thermodynamics to illustrate how phase boundary extrapolations to low temperatures can sometimes be shown to be in error. In addition, errors which may arise in the construction of phase diagrams that include higher order thermodynamic transitions (e.g. magnetic or atomic ordering) are briefly mentioned. These construction rules and comments should be of help to scientists who rely on phase diagrams in the development of materials. Also, we hope that it will be of help to those who utilize computer programs and compilations to display their modeled phase diagrams properly.

1. Introduction

Phase diagrams have been important tools in the study of materials for well over a century. Such diagrams display which phases are in equilibrium under the specific conditions in which a material may find itself under the influence of temperature, pressure, composition or any additional thermodynamic variables of the system. A phase can be defined as: "…a physically distinct homogeneous portion of a thermodynamic system delineated in space by a bounding surface, called an interphase interface, and distinguished by its state of aggregation (solid, liquid or gas), crystal structure, composition and/degree of order. Each phase in a material system generally exhibits a characteristic set of physical, mechanical and chemical properties and is, in principle, mechanically separable from the whole." [1]. When the thermodynamic parameters change, a phase may transform into one or more different phases. Phase diagrams indicate the thermodynamic parameters which can be altered to cause such phase changes.

In Section 2 of this paper, we first review some of the necessary characteristics of Pressure/Temperature phase diagrams for unary systems and discuss possible errors in their construction. Next, in Section 3, we discuss binary alloys and examine the following types of possible construction errors associated with them. We divide these types of construction errors into the following:

* Corresponding author.
E-mail addresses: laughlin@cmu.edu (D.E. Laughlin), massalski@cmu.edu (T.B. Massalski).

https://doi.org/10.1016/j.pmatsci.2020.100715
Received 14 May 2020; Received in revised form 8 July 2020; Accepted 9 July 2020
Available online 15 July 2020

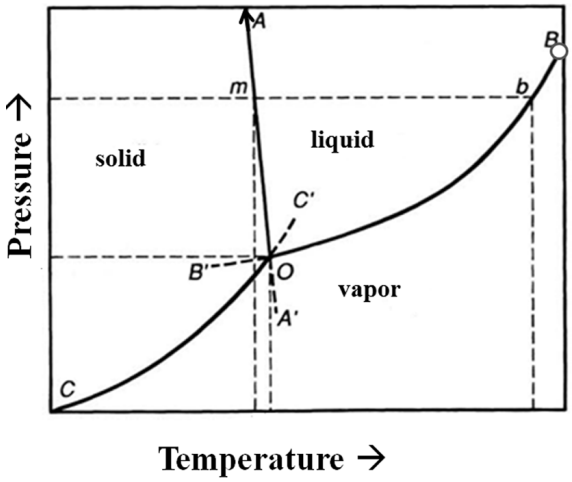

Fig. 1. A Pressure/Temperature equilibrium phase diagram of a one component system, drawn consistent with thermodynamic principles. Point B is a critical point and point O is a triple point.

1. Departures from the Gibbs Equilibrium Phase Rule
2. Incorrect Phase Boundary Configurations
3. Thermodynamically Improbable Aspects of some Phase Diagrams
4. Errors related to the Third Law of Thermodynamics
5. Incorrect constructions of Higher Order Phase Transitions

Recent progress in advanced computer programs and their use in calculations of phase stability indicates that more and more phase diagrams are being computed rather than determined experimentally. The need to integrate sound thermodynamic concepts into the computer programs which avoid producing phase diagrams, with improbable constructions is thus of increasing importance.

2. One component systems: Pressure/temperature diagrams

2.1. Introduction [2]

A Pressure/Temperature equilibrium phase diagram of a one component system which can exist in different states of aggregation is displayed in Fig. 1. In this diagram the liquid phase has a smaller molar volume than the solid phase. See Section 2.2.3, below. Such phase diagrams are commonly included in Physics, Chemistry, and Thermodynamics textbooks. The Pressure/Temperature phase diagrams indicate many important aspects of phase equilibria that need to be considered in a graphical display of a one component system. The corresponding molar thermodynamic energy functions and their natural independent thermodynamic variables (entropy, volume, pressure or temperature) are expressed as:

$$Internal\ \ energy : U = U(S, V) \tag{1a}$$

$$Enthalpy\ \ H = H(S, P) \tag{1b}$$

$$Helmholtz\ \ Free\ \ Energy\ \ A = A(T, V) \tag{1c}$$

$$Gibbs\ \ Free\ \ Energy\ \ G = G(T, P) \tag{1d}$$

Although phase diagrams of one component systems are typically displayed as Pressure/Temperature diagrams, other types of diagrams (e.g. Temperature/Volume for gases; Entropy/Temperature for condensed phases) are also used.

2.2. Specific features of pressure/temperature phase diagrams

2.2.1. Description of the phase diagrams

The Pressure/Temperature phase diagrams of one component systems have three types of regions indicating phase stability in their two dimensional plots. These are:

- *Areas*, in which only one phase is present when the system is in equilibrium. The phase which is present in equilibrium has two thermodynamic degrees of freedom, namely the temperature and the pressure. Both of these intensive thermodynamic variables can be altered in value without changing the phase which is present in equilibrium.

- *Lines (curves),* along which two phases coexist in thermodynamic equilibrium. States of a system whose pressure and temperature lie on a line have only one thermodynamic degree of freedom (either the temperature or the pressure). If one of these intensive thermodynamic variables is altered the other must change by a particular amount in order to retain the two phase equilibrium and thereby remain on the line.
- *Triple Points*, at which three phases are in thermodynamic equilibrium. Three phase equilibrium of one component systems has no thermodynamic degrees of freedom. The three phase equilibrium can only exist at the specific temperature and pressure associated with the triple point. Any change in one of the thermodynamic variables (P or T) will move the system into a single phase region.
- *Critical Points*, at which the two phase equilibrium between the vapor phase and its liquid phase ceases to exist. At and beyond such points the two phases become indistinguishable and should be considered as a single phase. The Gibbs Equilibrium Phase Rule can not be applied at critical points because such transitions are not thermodynamically first order.

2.2.2. Number of possible phases in equilibrium [3–6]

For a one component system, each phase has two thermodynamic variables, namely its temperature and pressure. Therefore, if there are Φ phases present, there are 2 Φ thermodynamic variables of the system.

The equations which must hold for equilibrium are:

$$T_\alpha = T_\beta = \cdots$$

$$P_\alpha = P_\beta = \cdots$$

$$\mu_\alpha = \mu_\beta = \cdots$$

where μ_i are the chemical potentials of the phases. Hence there are $3(\Phi - 1)$ equations or restrictions for equilibrium to be present. The difference between the number of thermodynamic variables and the number of restrictions imposed by equilibrium is defined as the degree of freedom, ($\mathscr{F}$) of the system. Hence for a one component system:

$$\Phi + \mathscr{F} = 3 \tag{2a}$$

This limits the number of possible phases in equilibrium in one component systems to a maximum of 3 (when $\mathscr{F} = 0$). As discussed above, if three phases exist in equilibrium they must do so at a specific temperature and pressure (i.e. the triple point in Fig. 1). Two phase coexistence (one degree of thermodynamic freedom) occurs along the lines of the diagram. Areas display the phase (two degrees of freedom) which is in equilibrium in those regions of the diagram.

Eq. (2a) is a special case of the Gibbs Equilibrium Phase Rule, namely of a one component system. For a system containing C components, each phase has $C + 1$ thermodynamic variables, namely the temperature, pressure and $C - 1$ composition variables. Thus the total number of thermodynamic variables of the C component system is $\Phi\ (C + 1)$.

The number of equations for equilibrium is now $(C + 2)(\Phi - 1)$ since the chemical potential of each component must be equal in all Φ phases. Subtracting the number of restrictions from the number of thermodynamic variables leads to the Gibbs Equilibrium Phase Rule for a C component system, namely:

$$\Phi + \mathscr{F} = C + 2 \tag{2b}$$

where:

- Φ is the number of phases which may coexist in equilibrium.
- $\mathscr{F}$ is the number of degrees of freedom of the system.
- C is the number of components of the system.

It can be seen that the maximum number of phases that can coexist in thermodynamic equilibrium in a C component system is $C + 2$.

2.2.3. Slopes of the two-phase equilibrium Lines

The slope of the curves (lines) of the Pressure/Temperature equilibrium diagrams for a one component system follow the Clapeyron equation for first order transformations, namely:

$$\frac{dP}{dT} = \frac{\Delta H}{T\Delta V} = \frac{\Delta S}{\Delta V} \tag{3}$$

where:

ΔH is the molar enthalpy change of the transformation
ΔS is the molar entropy change of the transformation
ΔV is the molar volume change of the transformation
and T is the temperature at which the slope is measured

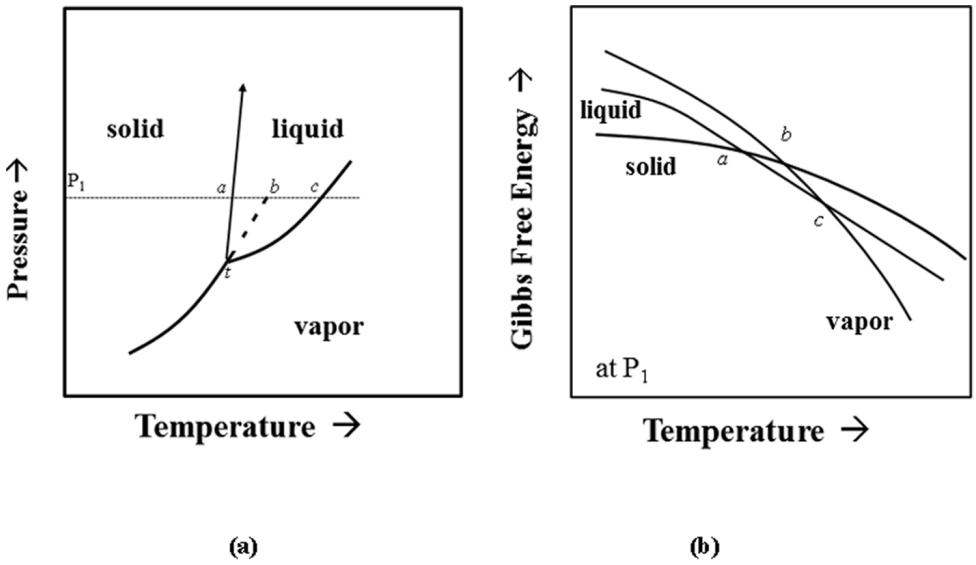

Fig. 2. (a) A Pressure/Temperature phase diagram for the three phases: solid, liquid and vapor. The metastable extension of the solid/vapor curve is seen to lie in the region where the liquid phase is stable. (b) Gibbs Free Energy versus Temperature curves for the three phases at P_1, showing that the two phase solid/vapor state at *b* is *metastable* with respect to the single phase liquid state.

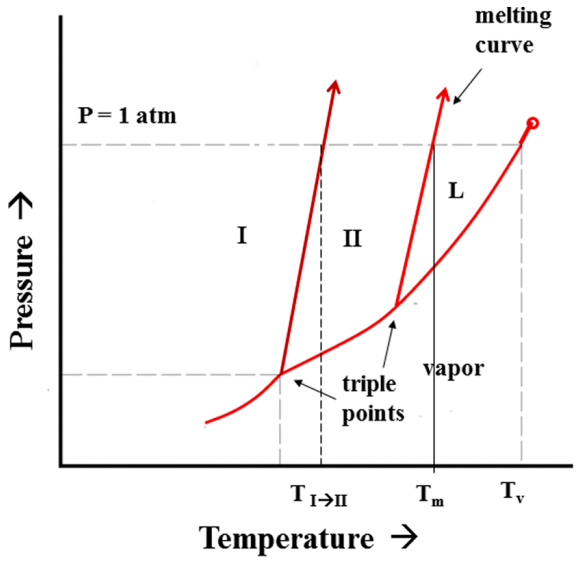

Fig. 3. A pressure/temperature phase diagram in which the solid phase displays allotropy. Two triple points exist in this phase diagram.

Changing from a condensed phase to the vapor phase requires the input of energy, and so in the solid/vapor and liquid/vapor transitions, ΔH is positive. These curves must therefore have positive slopes, since the vapor phase has a much larger molar volume than either of the condensed phases. The slope of the solid/liquid curve is usually positive as well, but there are known examples (*i.e.* H_2O) where the liquid has a smaller molar volume than the solid, giving rise to a negative slope of the solid/liquid curve.

2.2.4. Metastable extensions of the coexistence curves

Another feature of the Pressure/Temperature phase diagrams is that the extensions of the two phase coexistence curves through the triple point must go into the single phase region of the third phase which is present at the triple point. See the dashed curves *OC′*, *OB′* and *OA′* in Fig. 1 and the dashed curve *tb* in Fig. 2a. It can be seen in Fig. 2 that at a pressure larger than the triple point pressure, the extension of the solid/vapor curve (shown as the dashed curve *tb*) extrapolates into the single phase liquid region of the diagram. That this must be the case can be seen from the Gibbs Free Energy plots of the three phases at Pressure = P_1 (Fig. 2b). Gibbs free energy plots of the possible phases versus temperature determine the phase or phases which are in equilibrium at a temperature in question. As is shown in many textbooks [7–10,2], the Gibbs function G has a minimum value at equilibrium when the pressure is constant.

The stable phase at *b* in Fig. 2a is the liquid phase (it has the lowest Gibbs Free Energy, along *ac* of Fig. 2b) and the solid/vapor equilibrium can be seen to be *metastable* at this pressure. The curve therefore extrapolates into the single phase liquid region. This rule

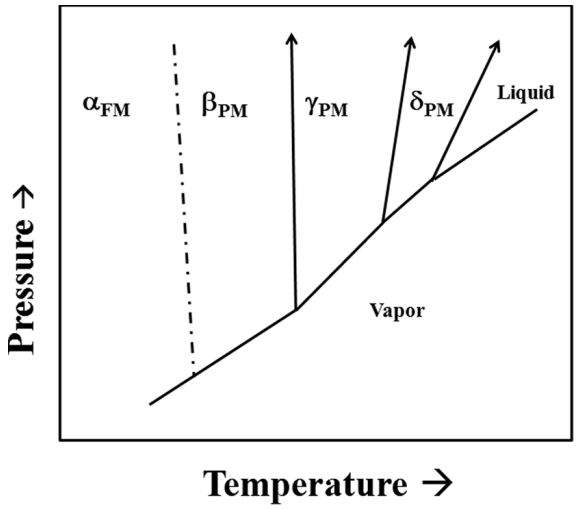

Fig. 4. A schematic Pressure/Temperature equilibrium phase diagram that displays a paramagnetic (β) to ferromagnetic (α) phase transition lines. Such higher order transitions are typically indicated by dot-dash curves.

is one of the Schreinemaker's rules [11].

2.2.5. Endpoints of the coexistence curves: the critical point

Fig. 1 also displays what is called a critical point (B), where the two existing phases (liquid and vapor) cease to be distinguishable and become a single phase. The phase in the region of higher temperature or pressure can be thought of as a dense vapor phase or as a liquid phase less dense than usual. Such critical points have been the study of chemists and physicists for more than a century and a half, since being discussed in detail by Andrews [12] and later modeled in the well known van der Waals equation [13].

There is no critical point associated the crystalline solid/liquid curve because those two phases (the crystal with discrete crystallographic symmetry and the liquid with full isotropy) cannot change from the one phase continuously to the other. Crystallographic symmetry is either present or it is not, so as soon as it is present, a phase change has occurred and must be so delineated on the phase diagram. For this reason the solid/liquid curve has an arrow attached to it in Fig. 1 to remind the reader that such two phase equilibria does not terminate at a *critical point*.

It should be noted that when a solid phase is present in the Pressure/Temperature equilibrium phase diagrams, it is implicitly assumed that it is a crystalline phase, since amorphous or glassy phases are not equilibrium thermodynamic phases.

2.2.6. Phase diagrams displaying solid state allotropy

Some Pressure/Temperature phase diagrams display more than one solid phase. Such systems are said to display allotropy. Each of the solid phases may have triple points associated with them. In the case displayed in Fig. 3, the low temperature solid phase produces a three phase equilibrium among the two solid phases and the vapor phase. The other triple point represents equilibrium among the solid II phase, the liquid and the vapor phase. Note that the curve displaying equilibrium of the phases I and II has an arrow attached to it to indicate that this equilibrium cannot end at a critical point since the different crystallographic symmetries of the allotropic phases do not allow for a continuous transformation.

2.2.7. Non-first order transformations

Some atomic disorder/order transformations as well as most magnetic transitions are not first order transitions, i.e. they are not the type of transitions that Gibbs utilized in his thermodynamic description of phases. Such transformations are sometimes called *second order* transitions (after Ehrenfest [14]), but are better designated as higher order or continuous transformations. At and above the transition temperature (called the Curie temperature for the paramagnetic to ferromagnetic transformation) the disordered phase is stable. Below the transformation temperature the ordered phase is stable. Such transformations should be delineated differently (in Fig. 4 as dot-dash) than the first order ones, to emphasize that they are not regions of two phase coexistence, as only the disordered phase is present along the curve. These lines are critical lines.

The phases on either side of the Curie curve are different phases in that they have different properties and symmetry. See ([15,16] for a discussion of this).

In Fig. 4, the intersection of the higher order transition line (Curie line) with the vapor curve is not a triple point, since at the point of intersection only the disordered solid phase (paramagnetic β phase) is present along with the vapor phase. If one were to apply the Gibbs Phase Rule at that point it would not be valid, since the point contains a higher order transition and therefore is not a first order transition.

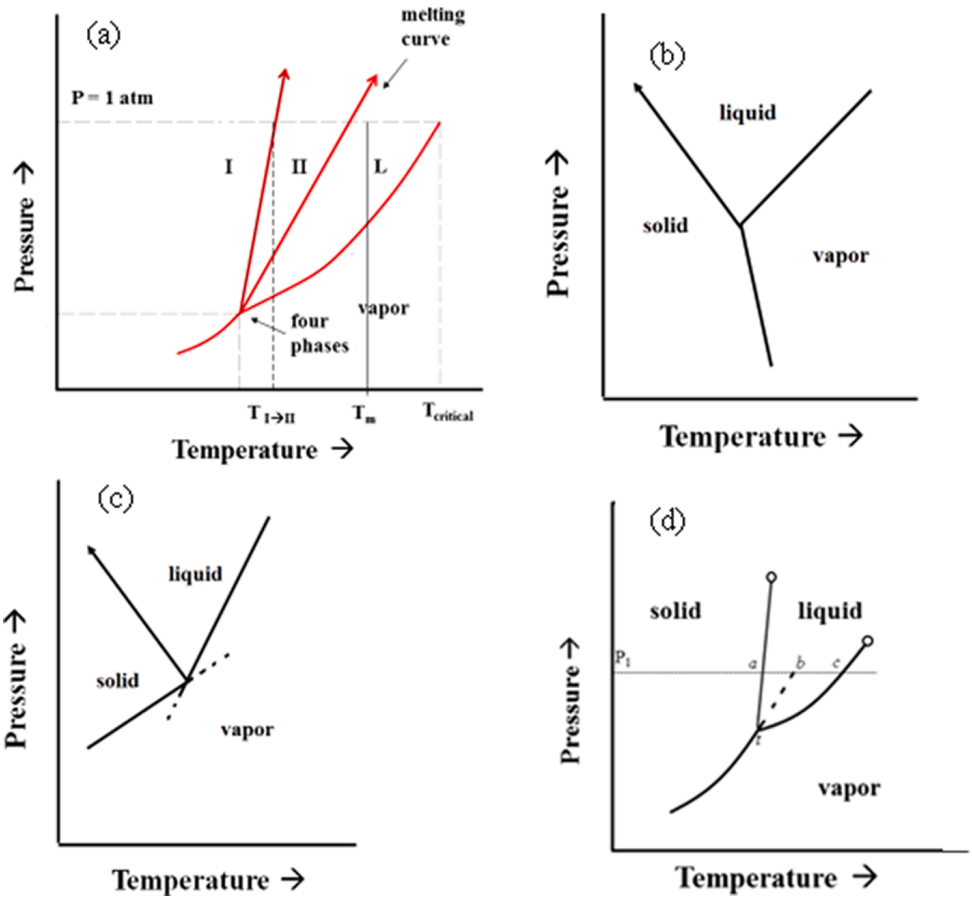

Fig. 5. Pressure/Temperature phase diagrams which display construction errors. In (a) four phases are shown to be in equilibrium. In (b) the slope of the solid/vapor equilibrium curve is shown to be negative. In (c) the extensions of the equilibrium two phase curves do not go into the proper single phase regions. In (d) an impossible critical point at the end of the solid/liquid curve is shown.

2.3. Possible errors in pressure/temperature diagrams

Examples of violations of the above thermodynamic features result in the following errors of construction as shown in Fig. 5.

1. More than three phases shown to coexist in equilibrium (Fig. 5a).
2. Slopes of a coexistence curve not consistent with the Clapeyron equation (Fig. 5b)
3. Metastable extensions of the two phase coexistence curves not extending into the proper single phase region (Fig. 5c)
4. A critical point for solid liquid or solid/solid coexistence curves (Fig. 5d).

3. Two component systems: Temperature/composition phase diagrams

3.1. Gibbs equilibrium phase rule constraints

When we study phase diagrams with more than one component associated with them we must include another thermodynamic variable in our description of the system, namely, the number of moles of *each* of the components. Eq. (1) now are written in terms of the total energy functions:

$$Internal\ \ energy: U = U(S, V, n_i) \tag{4a}$$

$$Enthalpy\ \ H = H(S, P, n_i) \tag{4b}$$

$$Helmholtz\ \ Free\ \ Energy\ \ A = A(T, V, n_i) \tag{4c}$$

$$Gibbs\ \ Free\ \ Energy\ \ G = G(T, P, n_i) \tag{4d}$$

where n_i is the number of moles of component *i,* that is present in the alloy.

The Gibbs free energy now has as its independent thermodynamic variables the temperature and pressure and number of moles of

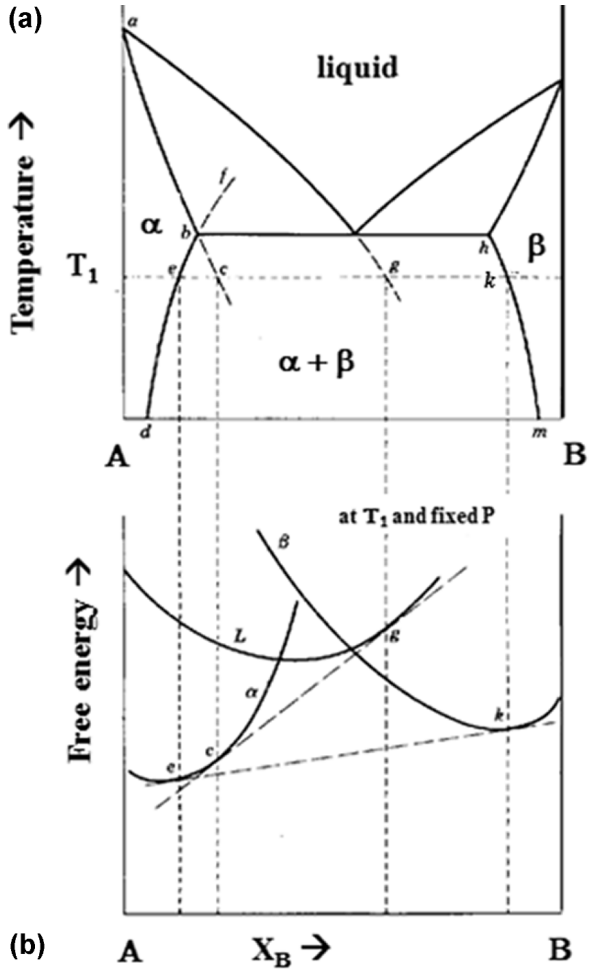

Fig. 6. (a) A constant pressure, Temperature/Composition binary equilibrium phase diagram of a system exhibiting an eutectic transformation. The three phase equilibrium is shown to be an invariant temperature in conformity to the Gibbs Equilibrium Phase Rule. The diagram shows the proper extensions of the two phase boundaries into adjacent two phase regions. (b) The free energy plots of the phases which show their relative positions. After [9].

each of the components. The thermodynamic conjugate to the number of moles is known as the chemical potential, denoted as μ_i. From the above it can be seen that:

$$\mu_i = \left(\frac{\partial U}{\partial n_i}\right)_{S,V,n_j} = \left(\frac{\partial H}{\partial n_i}\right)_{S,P,n_j} = \left(\frac{\partial A}{\partial n_i}\right)_{T,V,n_j} = \left(\frac{\partial G}{\partial n_i}\right)_{T,P,n_j} \tag{5}$$

These should not to be confused with the partial *molal* properties of the system, which are given as [7]

$$\left(\frac{\partial U}{\partial n_i}\right)_{T,P,n_j},\ \left(\frac{\partial H}{\partial n_i}\right)_{T,P,n_j},\ \left(\frac{\partial A}{\partial n_i}\right)_{T,P,n_j},\ \textit{and}\ \left(\frac{\partial G}{\partial n_i}\right)_{T,P,n_j}$$

It can be seen that only the partial *molal* Gibbs free energy is also a chemical potential.

A typical Temperature/Composition binary phase diagram (at constant pressure) is shown in Fig. 6a. As was the case for single component systems, the phase or phases in equilibrium for a certain combination of thermodynamic variables is determined from plots of the Gibbs free energy (Fig. 6b). The equilibrium phase or phases present as a function of composition of the system is determined by the lowest values of G.

Thus, at T_1,

- from B = 0 to B = *e*, the α phase is the stable phase
- from B = e to B = *k*, equilibrium consists of the two phase α plus β coexistance, determined by the common tangent construction.
- from B = *k* to B = 1, the β phase is the equilibrium phase.

At other temperatures, the free energy curves move with respect to each other and other combinations of equilibrium phases will be present.

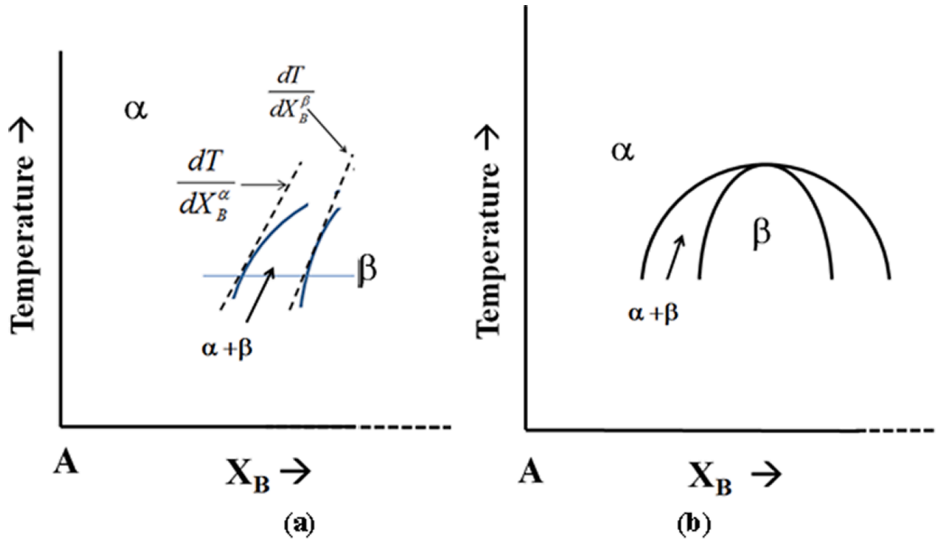

Fig. 7. (a) A partial Temperature/Composition phase diagram at constant pressure which displays the solvi of α and β phases which are in equilibrium. The slopes of the solvi are shown and can be determined by Eq. (6). (b) A continuation of the equilibrium diagram shown in (a) showing that when the two solvi intersect they do so at zero slope.

As was the case in the Pressure/Temperature phase diagrams there are three types of regions of equilibria: those that are areas, curves or points. These regions have specific thermodynamic characteristics that must be followed in equilibrium binary Temperature/Composition phase diagrams.

The *areas* denoted with one symbol are regions where there is only one phase present when the system is in equilibrium. The phase which is present has two thermodynamic degrees of freedom. These degrees of freedom are the temperature and the composition of the phase (remember that the pressure is constant). Small changes may be made in these variables without changing the equilibrium phase.

The *areas* denoted by two symbols are equilibrium regions of coexistence between two phases. In such regions only one thermodynamic degree of freedom exists. If for example the temperature is slightly changed, the composition of the two phases present must change in order to maintain equilibrium. If the composition of each of the phases were to change, there must be a change in temperature to maintain equilibrium.

Curves in the phase diagrams denote boundaries between differing phase regions (*ab, bf, fc, cg, gd* and *dc*). On passing through the curves (horizontally or vertically) the phases in equilibrium change. The curves denote the composition of the phase which is in both of the adjacent regions. Alloys existing on the curves (except for the horizontal invariant one) have one degree of thermodynamic freedom. For example if the temperature is changed the composition on the curve must be changed by a fixed amount to remain on the curve. It can be seen that single phase regions are separated by two phase regions except for the horizontal invariant line,

There are two types of regions with zero degrees of freedom ($\mathscr{F} = 0$) depicted on the constant pressure Temperature/Composition phase diagrams. The melting of either of the two pure components must be at a fixed temperature since the solid and liquid phases coexist during first order phase transformations. The constant pressur Gibbs Equilibrium Phase Rule for a binary system (C = 2) and the number of phases present is 2 (Φ = 2) shows that $\mathscr{F}$ is 0. The other region with zero degrees of freedom is the horizontal line which depicts the composition of the three phases which coexist in equilibrium at a fixed temperature. The constant pressure Gibbs Equilibrium Phase Rule also shows this to be the case, as Φ = 3 and C = 2, leaving $\mathscr{F}$ to be 0. This invariant coexistence line (representing three phases in equilibrium, namely α, β and L) lies between regions of two phase equilibria.

3.1.1. Possible errors in the construction of temperature/composition phase diagrams

Examples of violations of the above thermodynamic features include the following errors of construction:

a. Melting of the constituents not being denoted as a single temperature.
b. The three phase invariant line not being denoted as being horizontal.
c. A horizontal line not delineating a three phase equilibrium
d. More than three phases depicted as coexisting in equilibrium,
e. Two two-phase regions in contact with each other (except for the ones in contact with a horizontal three phase region).
f. Phase boundaries that are shown to end within the diagram
g. Two phase regions not bounded by single phase regions except at an invariant temperature.

Some of these as well as other examples of phase diagram construction errors are displayed in Fig. A.1 of Appendix A (a at A; *b* at N; *c* at G; *d* at S and *f* at O). Earlier compilations of phase diagram construction errors may be found in [8–10].

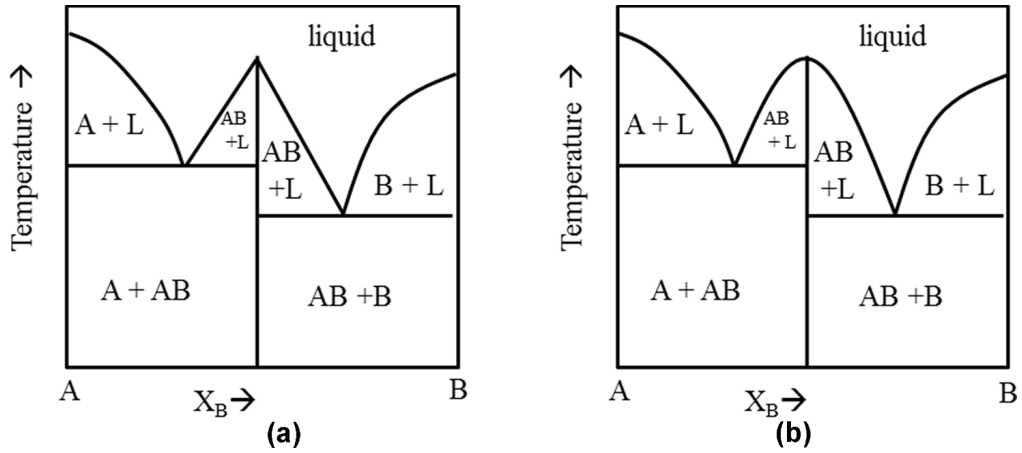

Fig. 8. (a) A constant pressure Temperature/Composition phase diagram which displays an error in the depiction of the two liquidi curves at the congruent point of the compound. (b) A phase diagram demonstrating the proper depiction of the liquidus at the congruent point in that the curves at a maximum with zero slope. In these diagrams it is assumed that the solubility of B in either the liquid or solid phase of A and the solubility of A in either the liquid or solid phase B is very small and is not depicted on the diagram.

3.1.2. Slopes of the temperature/composition curves at congruent points

Another constraint imposed by equilibrium thermodynamics on the possible configuration of Temperature/Composition phase diagrams has to do with the slopes of coexistence curves in a binary diagram. In Fig. 7a, the two coexistence boundaries between the α phase and the β phase are shown and the slopes of the curves at a fixed temperature and pressure are displayed. The following two equations of the coexistence curves are adopted from Wagner [17]. See also [18] where the equations are referenced to an earlier paper by Konovalov and are denoted as the Gibbs-Konovalov equations.

$$\left(\frac{dT}{dX_B^{\alpha}}\right) = \frac{(X_B^{\beta} - X_B^{\alpha})T\left(\frac{\partial^2 G^{M,\alpha}}{\partial (X_B^{\alpha})^2}\right)}{\left\{X_A^{\beta}\Delta H_A^{0(\alpha\rightarrow\beta)} + X_B^{\beta}\Delta H_B^{0(\alpha\rightarrow\beta)}\right\}}$$

and (6)

$$\left(\frac{dT}{dX_B^{\beta}}\right) = \frac{(X_B^{\beta} - X_B^{\alpha})T\left(\frac{\partial^2 G^{M,\beta}}{\partial (X_B^{\beta})^2}\right)}{\left\{X_A^{\alpha}\Delta H_A^{0(\alpha\rightarrow\beta)} + X_B^{\alpha}\Delta H_B^{0(\alpha\rightarrow\beta)}\right\}}$$

where:

$\left(\frac{dT}{dX_B^{\alpha}}\right)$ and $\left(\frac{dT}{dX_B^{\beta}}\right)$ are the slopes of the two curves, respectively,

X_B^{α} and X_B^{β} are the B compositions of the α and β phases,

T is the temperature of the system

$\left(\frac{\partial^2 G^{M,\alpha}}{\partial (X_B^{\alpha})^2}\right)$ and $\left(\frac{\partial^2 G^{M,\alpha}}{\partial (X_B^{\beta})^2}\right)$ are the second derivatives of the Gibbs free Energy of mixing of the α and β phases, and

$\Delta H_A^{0(\alpha\rightarrow\beta)}$ and $\Delta H_B^{0(\alpha\rightarrow\beta)}$ are the enthalpies of transition of the α to β phase.

Since the denominators of both of Eq. (6) are related to the heats of formation of the high temperature α phase to the low temperature β phase, they are negative (exothermic). For the solvi drawn in Fig. 7a, the slopes of the curves are positive, since the numerator is negative($X_B^{\beta} - X_B^{\alpha} < 0$). It can be seen from the equations that if the coexistence curves intersect, they must do so with zero slope since at their intersection, $X_B^{\beta} = X_B^{\alpha}$. This yields a zero slope for both of the solvi at their intersection. Hence the phase diagram would have the configuration shown in Fig. 7b. That is, the curves should intersect with zero slope at a maximum in the Temperature/Composition phase diagram. Such points are often called congruent points in that the compositions of the phases which are involved in the transformation are the same.

A phase diagram which displays a congruently melting intermediate phase cannot be thought of as consisting of two juxtaposed simple eutectics as shown in in Fig. 8a, since the two liquid/compound phase boundaries must meet at zero slope and be drawn as shown in Fig. 8b. If a congruently melting compound exists in a system A-B, additions of infinitesimally small amounts of either A or B elements to the compound will initially neither lower or raise the melting temperature.

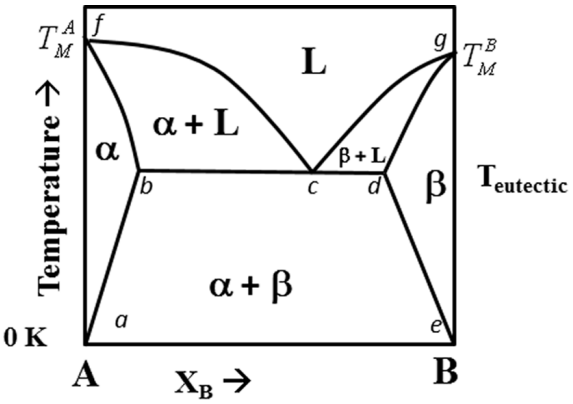

Fig. 9. A binary phase diagram which displays phase boundaries which do not have slopes approaching +/− infinity at zero K.

3.2. Phase boundary extrapolation errors of construction

Fig. 6 shows that the extrapolation of the two phase boundaries (*abc*, *ebf*, etc.) enter adjacent two phase regions. That this must be the case can be seen from the accompanying free energy vs. composition curves for the respective phases.

At temperature T_1, in Fig. 6a, which is just below the eutectic temperature, the extension of the α/liquid solidus (*ac*) and the α/liquid liquidus (*ag*) extrapolate into the α/β two phase region. The composition of the metastable liquid phase in equilibrium at *c* has a greater solubility in α than that of the equilibrium β phase, *e*. This occurs because the free energy curve of the liquid (shown in Fig. 6b) is less negative that that of the β phase. This causes its common tangent with the α free energy curve to occur at a larger value of X_B than the common tangent of the stable phase free energy curve with that of the α free energy curve. These are general features of metastable phases which necessitates that all extensions of phase boundaries into regions in which they are not stable, should display these characteristics. See a violation of this construction at E in Fig. A.1 in Appendix A.

3.3. Improbable binary phase diagram constructions

The construction errors discussed in Sections 3.1 and 3.2 were explicit violations of the Gibbs Equilibrium Phase Rule or construction violations concerning phase equilibria. In the course of compiling the three volume reference book on binary phase diagrams [19], Okamoto and Massalski noticed many cases of phase boundary features that did not directly violate any thermodynamic laws or equations, but in order for the diagrams to be valid, very drastic changes in some of the thermodynamic functions would have to have been present. They termed these "thermodynamically improbable" phase diagram constructions [20]. These improbable constructions are often subtle in nature, and a diagram may look to have no errors, until some quantitative thermodynamic calculations are performed. The opposite is also possible: a diagram may look "strange" but contain no errors in construction. A good example of this is a solvi displaying retrograde solubility.

3.3.1. Slopes of the temperature/composition curves at low temperatures

The inverse of the slopes of the Temperature/Composition plots for Raoultian solutions can be derived from Eq. (7) and have been shown by Lupis and Gayle [21,22] to be:

$$\frac{dX_B^{\alpha}}{dT} = \frac{(X_A^{\alpha}X_B^{\alpha})}{(X_B^{\alpha}-X_B^{\beta})RT^2}\cdot\left\{X_A^{\beta}\Delta H_A^{0(\alpha\to\beta)} + X_B^{\beta}\Delta H_B^{0(\alpha\to\beta)}\right\} = \frac{\left\{X_A^{\beta}\Delta H_A^{0(\alpha\to\beta)} + X_B^{\beta}\Delta H_B^{0(\alpha\to\beta)}\right\}}{(X_B^{\alpha}-X_B^{\beta})T\left(\frac{\partial^2 G^{M,\beta}}{\partial\left(X_B^{\beta}\right)^2}\right)}$$

$$\frac{dX_B^{\beta}}{dT} = \frac{(X_A^{\beta}X_B^{\beta})}{(X_B^{\beta}-X_B^{\alpha})RT^2}\cdot\left\{X_A^{\alpha}\Delta H_A^{0(\beta\to\alpha)} + X_B^{\alpha}\Delta H_B^{0(\beta\to\alpha)}\right\} = \frac{\left\{X_A^{\alpha}\Delta H_A^{0(\beta\to\alpha)} + X_B^{\alpha}\Delta H_B^{0(\beta\to\alpha)}\right\}}{(X_B^{\beta}-X_B^{\alpha})T\left(\frac{\partial^2 G^{M,\alpha}}{\partial\left(X_B^{\alpha}\right)^2}\right)} \quad (7)$$

These equations show that near T = 0 K, the slopes of the solvi (viz. $\frac{dT}{dX_B^{\alpha}}$ and $\frac{dT}{dX_B^{\beta}}$) approach plus and minus infinity respectively. Thus a diagram such as shown in Fig. 9 is incorrect at the low temperature limit.

3.3.2. Slopes of the solvi near the component melting temperature

Near the melting points of the elements A and B Eq. (8) are written in terms of the elemental solid phases (α or β) and the liquid phase, L. These are shown below for component B in the α and L phases.

$$\frac{dX_B^{\alpha}}{dT} = \frac{(X_A^{\alpha}X_B^{\alpha})}{(X_B^{\alpha}-X_B^{L})RT^2}\cdot\left\{X_A^{L}\Delta H_A^{0(\alpha\to L)} + X_B^{L}\Delta H_B^{0(\alpha\to L)}\right\} \quad (8)$$

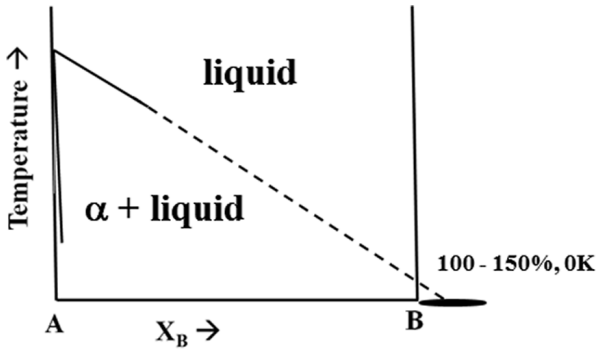

Fig. 10. A portion of a constant Pressure Temperature/Composition binary diagram showing that the initial slope of the liquidus curve for a system displaying very small sold state solubility, projects to a region in the vicinity of 100–115% B at 0 K.

$$\frac{dX_B^L}{dT} = \frac{(X_A^L X_B^L)}{(X_B^L - X_B^\alpha)RT^2} \cdot \left\{ X_A^L \Delta H_A^{0(L\to\alpha)} + X_B^L \Delta H_B^{0(L\to\alpha)} \right\}$$

The difference between these 2 equations is the initial difference in the inverse values of the slope of the solidus and liquidus curves.

$$\frac{dX_B^\alpha}{dT} - \frac{dX_B^L}{dT} = \frac{(X_A^\alpha X_B^\alpha)}{(X_B^\alpha - X_B^L)RT^2} \cdot \left\{ X_A^L \Delta H_A^{0(\alpha\to L)} + X_B^L \Delta H_B^{0(\alpha\to L)} \right\} - \frac{(X_A^L X_B^L)}{(X_B^L - X_B^\alpha)RT^2} \cdot \left\{ X_A^L \Delta H_A^{0(L\to\alpha)} + X_B^L \Delta H_B^{0(L\to\alpha)} \right\}$$

After rearranging and cancelling terms the difference simplifies to:

$$\frac{dX_B^\alpha}{dT} - \frac{dX_B^L}{dT} = \frac{(X_B^\alpha)}{(X_B^\alpha - X_B^L)RT^2} \cdot \left\{ \Delta H_A^{0(\alpha\to L)} \right\} - \frac{(X_B^L)}{(X_B^\alpha - X_B^L)RT^2} \cdot \left\{ \Delta H_A^{0(\alpha\to L} \right\} \tag{9}$$

$$\frac{dX_B^\alpha}{dT} - \frac{dX_B^L}{dT} = \frac{\Delta H_A^{0(\alpha\to L)}}{RT^2} = \frac{\Delta S_A^{0(\alpha\to L)}}{RT_M} \tag{10}$$

It can be seen that this difference in the inverse slopes depends only on the heat of solidification (enthalpy of fusion) of the solvent (element A) and the melting point of element A.

If the solubility B in the solid is negligible, the slope of the liquidus is:

$$\frac{dT}{dX_B^L} = -\frac{RT_M}{\Delta S_A^{0(\alpha\to L)}} \tag{11}$$

This is a version of the van't Hoff relationship.

The heat of solidification divided by the melting point is the entropy of solidification. For FCC metallic elements that obey Richard's Rule, the entropy of solidification is about −9.6 J/K. For BCC metallic elements the entropy of solidification is about −8.35 J/K. Thus, as reported by Okamoto and Massalski for phase diagrams where the solubility of component B in the solid is negligible, the initial slope of the liquidus should project to between 100 and 115 %B at 0 K. See Fig. 10.

If there is solid solubility of B in α, the projection of the initial slope needs to accommodate this since the difference in slopes now contains the slope of the solidus curve. Okamoto and Massalski have shown how this can be accomplished [20].

This example shows that although a phase diagram may look to be in order, the application of straight forward thermodynamic relationships may show that they are not be properly drawn if they do not comply with the extrapolation discussed above and displayed in Fig. 10.

3.4. Construction errors related to the Third Law of Thermodynamics

The Nernst-Planck-Simon version, of the Third Law of Thermodynamics, can be summarized as: the entropy of all substances in internal thermodynamic equilibrium approaches zero, as the temperature approaches 0 K, and is independent of pressure, external fields or state of aggregation [23]. This version of the Third Law can be applied to the various aspects or subsystems of the material (e.g. spin systems, vibrational and rotational states, etc.) provided they are in thermodynamic equilibrium.

Thus, the configurational aspects of the entropy of phases in equilibrium should approach zero as the zero in temperature is approached. This means that the ground state of alloys should consist of pure elements, stoichiometric compounds, and combinations of these phases which have zero configurational entropy at 0 K. There should be no solid solubility of elements or compounds which are in thermodynamic equilibrium at 0 K.

Over the past decade or so several authors [24,25,23] have applied the Third Law of Thermodynamics to phase equilibria at low temperatures. In this section we summarize their findings and specify errors that should be avoided in the construction of equilibrium binary phase diagrams, specifically with respect to the depiction of low temperature equilibrium.

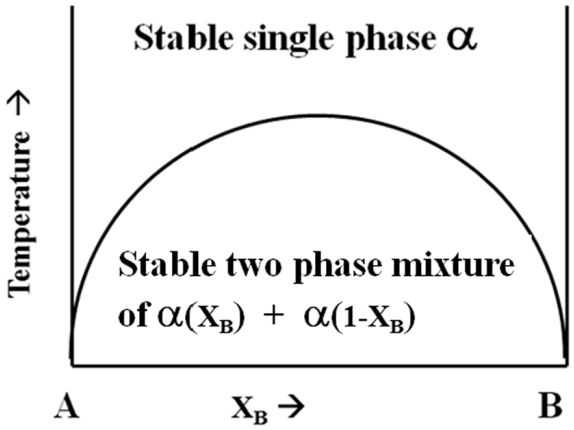

Fig. 11. A schematic constant pressure temperature/composition phase diagram of a system exhibiting regular solution behavior with positive deviation from ideality. The regular solution model (with positive deviation from ideality) is seen to be in conformity with the third law of thermodynamics at low temperatures. The two phase miscibility gap ends at the pure elements and the slope of the phase boundaries at pure A and B have ± infinite slopes.

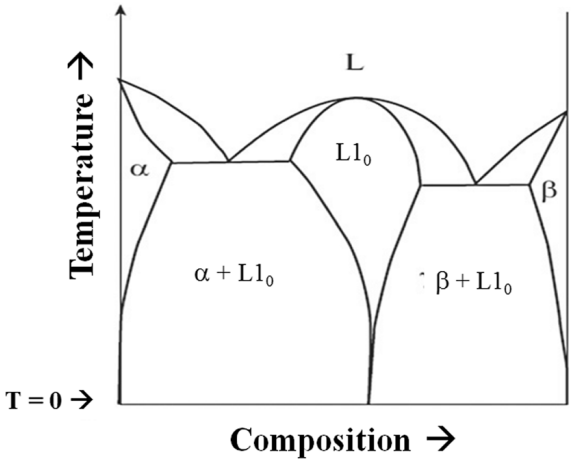

Fig. 12. A portion of a binary phase diagram at constant pressure that exhibits an ordered intermediate phase, ($L1_0$). The phase boundaries of the ordered phase meet at 0 K with infinite slopes (after Federov, [25]).

3.4.1. A regular solution

The regular solution model is a good place to start our discussion. This model solution with positive heats of mixing give rise to a low temperature diagram as shown in Fig. 11. It can be seen that as the temperature approaches 0 K the solid state solubility decreases until at 0 K the solubility is zero. The ground state for this simple solution is one composed of pure A and pure B phases. For a miscibility gap situation both phases must have the same crystal structure, namely that of the high temperature phase.

The equation for the miscibility gap [21] modeled as a regular solution is:

$$ln(\frac{X_B}{X_A}) = \frac{2T_C}{T}(X_B - X_A)$$

From this it can be determined that the initial slopes of the phase boundaries at A and B are $+\infty$ and $-\infty$ respectively. This is due to the initial infinite slope of the entropy of mixing curves at the pure A and pure B compositions.

3.4.2. Ordered intermetallic phases

When an ordered intermetallic phase exists in the middle regions of a binary phase diagram it has similar constraints placed upon it by the Third Law of Thermodynamics. In particular at low temperatures it must exist in a stoichiometric form with zero solubility of either of the components. This allows the atomic order parameter to attain the value of unity at equilibrium at zero K. Thus, the corresponding aspect of the entropy is able to approach zero at 0 K, and satisfy the Third Law dictates. An example of such a diagram is shown in Fig. 12. The slope of the solvus curves of the ordered phase is infinite in approaching 0 K. This is so because the ordered phase acts as a single component. Thus, when approaching 0 K its solvi must exhibit infinite slopes (negative on the solute lean side and positive on the solute richer side of the stoichiometric composition).

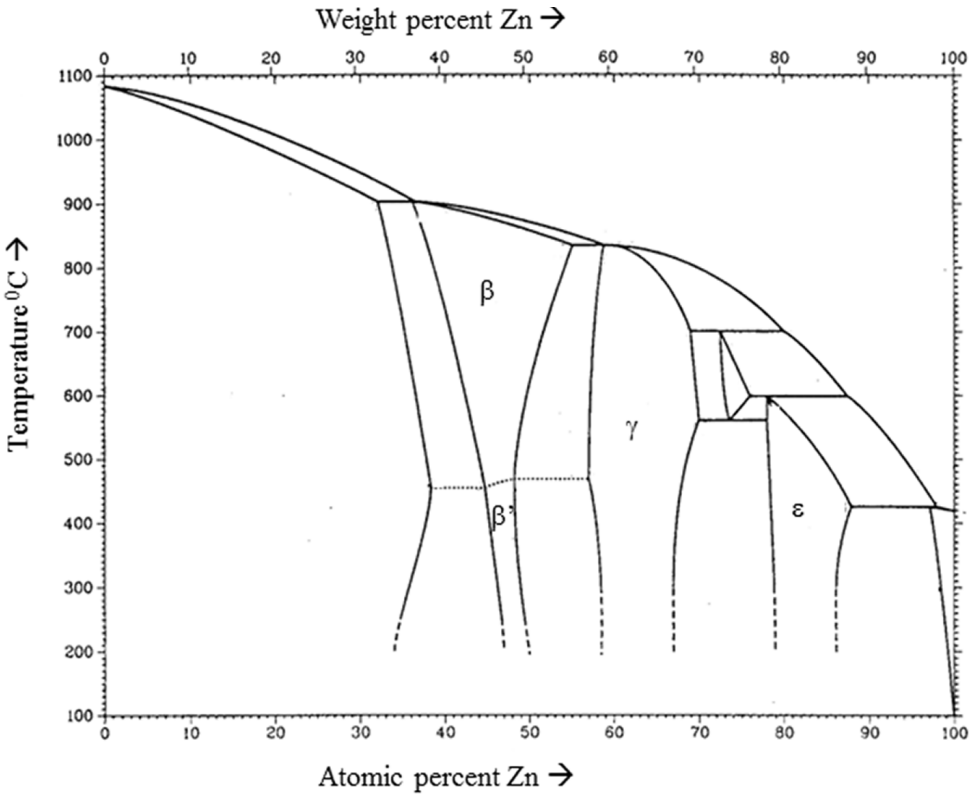

Fig. 13. The Cu Zn phase diagram that is shown in many compilations of phase diagrams. The intermetallic phases β′ γ and ε do not appear to extrapolate to a single composition at 0 K and the solvi of Zn in Cu does not project to 0% Zn at 0 K. After [19].

3.4.3. *Paramagnetic phases*

Phases comprised of components that exhibit magnetic spins are paramagnetc at elevated temperatures. However, they must order magnetically as the temperature is lowed. For alloys with exchange interactions this will result in one of the well-known magnetically ordered phases (ferromagnetic, antiferromagnetic or ferrimagnetic). If the exchange energy is very small or absent, the paramagnetic phase may continue to exist to very low temperatures, following the Curie Law. However, before the zero in temperature is reached such parmagnetic phases will order because of the interaction among their dipole moments. Such ordering usually produces anti-ferromagnetic structures.

3.4.4. *Some common construction errors at low temperature*

3.4.4.1. Alloys which seem to exhibit non-zero configurational entropy. A phase diagram like the Cu-Zn diagram shown in Fig. 13 has many potential Third Law construction errors [19]. The projected large solid solubility at low temperature for the Cu solid solution is readily seen (predicting Zn solubility in Cu at very low temperatures). If the β' phase is the stable phase with the lowest Zn content, its solvus curve must go to zero in composition at zero K, and its slope should be infinite. Thus, its extension shown in the diagram must be corrected to show either zero solubility or perhaps the existence of another phase at lower temperatures. This case is also an example of an improbable construction.

The large solubilities of the β′, γ and ε intermediate compound phases also should close to a point at zero K. Their phase boundaries are drawn with nearly vertical slopes leaving little chance for them meet this condition.

3.4.4.2. Low temperature equilibrium of a two-component ferromagnetic system. A schematic phase diagram of Co-Ni shown in Fig. 14 is incomplete as displayed. One possible correction to the phase diagram is shown in Fig. 15. Here the 0 K phase equilibria is shown to consist of the two ferromagnetic phases: pure Co (ε, hexagonal structure) and pure Ni (α', rhombohedral structure). The two phase region has first order phase boundaries, because they separate ferromagnetic phases of different structures (an HCP based structure and a FCC based structure) that can not transform into each other continuously. The transformations are likely to be sluggish, thereby hindering the obtaining of low temperature equilibrium. See [16] for a more detailed discussion.

3.5. *Construction of phase diagrams containing higher order phase transitions*

In the two-component systems discussed above the thermodynamic energy functions were functions of three independent variables, namely temperature, pressure and mole fraction of one of the components. When a magnetic field, $\mathscr{H}$, is present, the energy

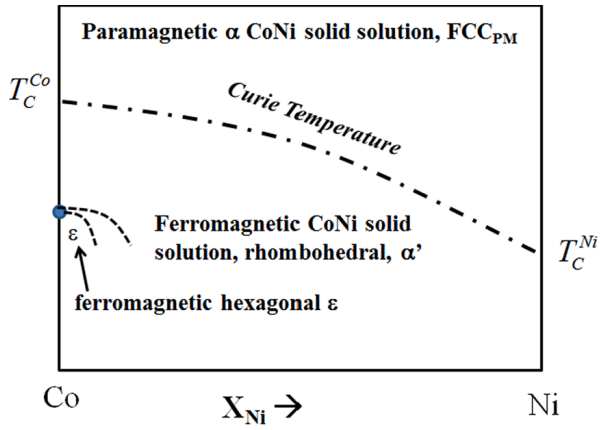

Fig. 14. Schematic Co Ni binary phase diagram. The dashed curves represent regions that have not been completely established.

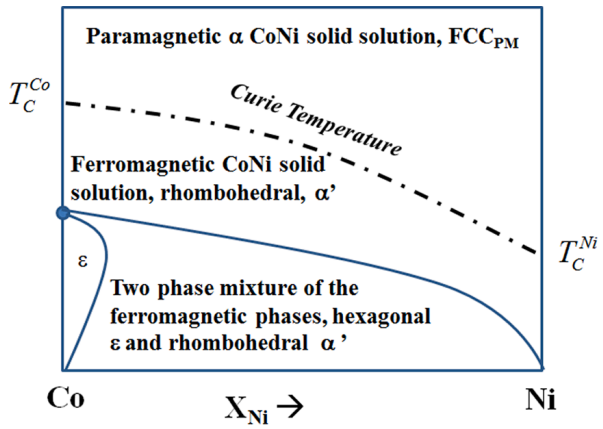

Fig. 15. A suggested schematic of the constant pressure Co Ni binary phase diagram which is in conformity with the Third Law of Thermodynamics. Note that the low temperature phases are pure Co and Ni with ferromagnetic ordering.

functions must include another independent thermodynamic variable, either the field $\mathscr{H}$ or its thermodynamic conjugate variable, the magnetization, $\mathscr{M}$. The following is one scheme that it used for the energy functions in the presence of a magnetic field. See [2].

$$\text{Internal energy: } U = U(S, V, n_i, \mathscr{M}) \tag{11a}$$

$$\text{Enthalpy: } H = H\ (S, P, n_i, \mathscr{H}) \tag{11b}$$

$$\text{Helmholtz Free Energy: } A = A\ (T, V, n_i, \mathscr{M}) \tag{11c}$$

$$\text{Gibbs Free Energy: } G = G\ (T, P, n_i, \mathscr{H}) \tag{11d}$$

This increase in the number of independent thermodynamic variable entails an increase in the number of degrees of freedom of the system, which allows for more phases to be in equilibrium within the system. This is so even if the phases are not ferromagnetic. When a magnetic field is applied to the system the equilibrium phase boundaries move in such a way as to increase the regions of stability of the phase or phases that have the greater magnetic susceptibilities [16].

3.5.1. *Curie temperature line*

We have already encountered a binary phase diagram with stable ferromagnetic phases in Fig. 15. The dot-dash line connecting the Curie temperatures of the pure components (Co and Ni) corresponds to the limit of stability of the magnetically disordered solid solution paramagnetic CoNi phase. Below that line, the high temperature cubic, magnetically disordered paramagnetic phase transforms to a ferromagnetic, rhombohedral solid solution whose structure is based on the FCC structure. The fact that a line exists between the stability regions of two single phases regions would be a violation of the Gibbs Equilibrium Phase Rule if the transition were of thermodynamic first order. However, magnetic transitions usually are of higher order and that is the case in this diagram for the paramagnetic to ferromagnetic transition in the CoNi system. At the Curie temperature, the equilibrium phase is the paramagnetic phase. As stated in the discussion of Fig. 15, the solid boundaries of the two phase equilibrium of the ε_{FM} and α'_{FM} phases are not

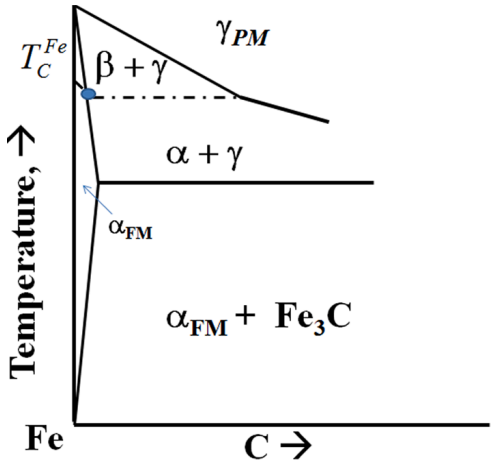

Fig. 16. Schematic of a portion of the metastable Fe-C constant pressure Temperature/Composition phase diagram showing the intersection of the Curie line with the two phase field. This line produces two phase regions separated by a horizontal line (*dot-dash*) which denotes the Curie temperature of the α_{FM} phase which is saturated with C. In the Figure, β represents the paramagnetic version of the BCC phase of Fe.

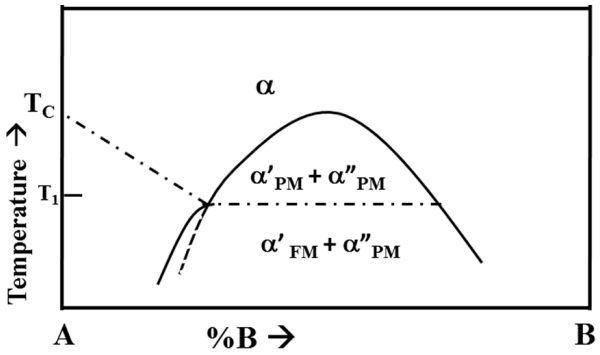

Fig. 17. A constant pressure schematic Temperature/Composition phase diagram showing the intersection of the Curie temperature curve with a miscibility gap. The horizontal line is the Curie temperature of alloys within the two phase field. The *dot-dash* line is the Curie curve and the dashed line is the metastable continuation of the miscibility gap of the two paramagnetic phases. On the horizontal line the phases in equilibrium are α'_{PM} and α''_{PM} (after Meijering [26]).

magnetic transitions, but structural ones and therefore are drawn as first order boundaries.

3.5.2. The case of Fe-C phase diagram

Sometimes the Curie line intersects boundaries of two phase regions in the Temperature/Composition phase diagram. Such is the case in the Fe-C phase diagram shown schematically in Fig. 16. The Curie temperature of the low temperature α_{FM} phase intersects the two phase γ/ferrite boundary in Fe-C phase diagram. An interesting feature is the horizontal Curie line. This line must be present because the phases in equilibrium with the γ phase are different above and below the line. Below the horizontal Curie line the γ phase is in equilibrium with the ferromagnetic α phase. Above the horizontal Curie line the γ phase is in equilibrium with the cubic, paramagnetic β phase. This means that the free energies of the α and β phases are different and thus the common tangent of their respective free energy plots with that of the γ_{PM} (FCC) phase would also differ. Hence at their intersection the slopes of the BCC based phase solvus and the γ_{PM} solvus would change slightly. These small changes are not usually displayed in phase diagrams but they should be present, albeit very small. In the phase diagram a slight change in the γ phase solvi is depicted, as this change was often displayed in early 20th century Fe-C phase diagrams. See [15,16] for a discussion of this effect as well as the historical precedence of calling the paramagnetic BCC phase of Fe, the β phase.

3.5.3. Intersection of a Curie curve with a miscibility gap

Another interesting phase diagram containing a higher order transistion was presented by Meijering [26] in a paper in which various effects that occur when the Curie temperature curve of a ferromagnetic transformation intersects a miscibility gap in a binary phase diagram were discussed. Fig. 17 is adopted from Fig. 1 of his paper. It shows a miscibility gap in which the high temperature paramagnetic α phase decomposes into two paramagnetic phases of the same crystal structure. It can be seen that when the Curie curve intersects the miscibility gap, an indentation appears in the phase boundary of the miscibility gap (exaggerated in the figure). This occurs because at the point of intersection the free energy curve of a ferromagnetic phase departs from that of the double hump free

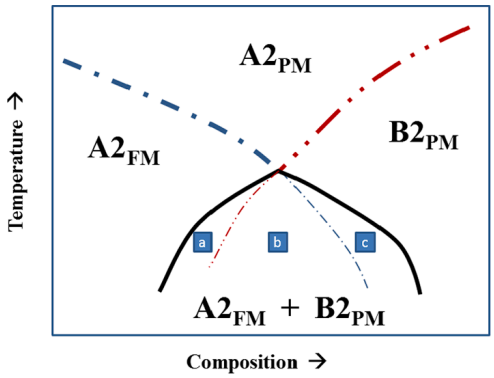

Fig. 18. A constant pressure schematic phase diagram of an alloy system exhibiting a bicritical point. The dot-dash curve represents the magnetic Curie curve of the A2 phase and the dot-dot-dash curve represents the higher order atomic ordering transition curve for the A2 phase. The solid curves are first order phase boundaries of the equilibrium two phase region comprised of the $A2_{FM}$ and $B2_{PM}$ phases.

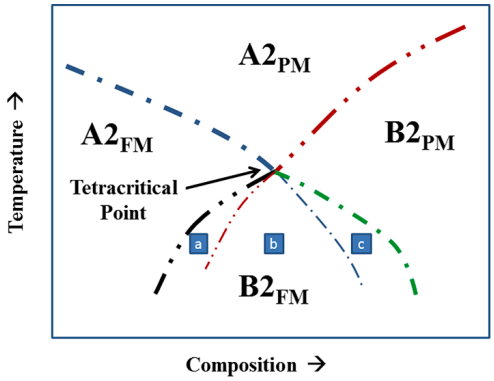

Fig. 19. A constant pressure schematic phase diagram of an alloy system exhibiting a tetracritical point. The phases which occupy the four single phase regions are delineated. The dot-dash curves represent magnetic Curie curves, and the dot-dot-dash curves represent higher order transition atomic ordering curves. The thinner curves are extrapolations of the high temperature higher order transition curves.

energy curve of the disordered phases of the miscibility gap. The common tangent construction produces a phase with a slightly less solubility of B in the ferromagnetic phase than in the paramagnetic phase at the temperature of the intersection. The gap is now divided into two regions: the upper region, with the α'_{PM} and α''_{PM} phases in equilibrium and the lower region with the α'_{FM} and α''_{PM} phases present in equilibrium. The horizontal line between these two-two phase regions is the Curie temperature of the ferromagnetic phase which forms at the intersection with the miscibility gap. As in the case of the Fe-C diagram (Fig. 16), the horizontal line is not a three phase invariant line, since only the two paramagnetic phases exist along it. A slight indentation also exists on the B rich side of the miscibility gap but is not displayed because it is usually too small to be observed.

3.5.4. Intersection of two higher order phase transitions curves

When two higher order transition lines intersect there are two basic topologies of the diagrams which may arise. We discuss here one magnetic higher order transition (PM → FM) depicted by a dot-dash line and one higher order atom ordering transition (A2 → B2) depicted by a dot-dot-dash line.

3.5.4.1. Bicritical point. A diagram with a *Bicritical* point is depicted in Fig. 18. Below the intersection of the two higher order transitions lines (the bicritical point) there is a two phase equilibrium between a ferromagnetically ordered phase ($A2_{FM}$) and a paramagnetic atomically ordered phase ($B2_{PM}$).

The solid boundary lines are not higher order lines and should not be depicted as dashed lines since they represent the boundaries of first order transformations. Since the low temperature ordered phases cannot exist above their respective higher order transition lines, there are no construction rules about extensions of their boundaries into other phase fields.

Alloys slowly cooled from the $A2_{FM}$ phase to region "a" or alloys slowly cooled from $B2_{PM}$ to region "c" must undergo the first order transformations (precipitation) before attaining the two phase equilibrium state. Of course the transformations away from equilibrium may occur continuously (for example in a direct quench from $A2_{PM}$ to region "b" which is below the extension of the lines of instability of the transformations) but since such transformations are away from their equilibrium transition temperatures, they are not designated as higher order transformations. It is important to remember that all higher order transformations (which occur in equilibrium) are continuous but not all continuous transformations (for example those occurring away from equilibrium) are higher order!

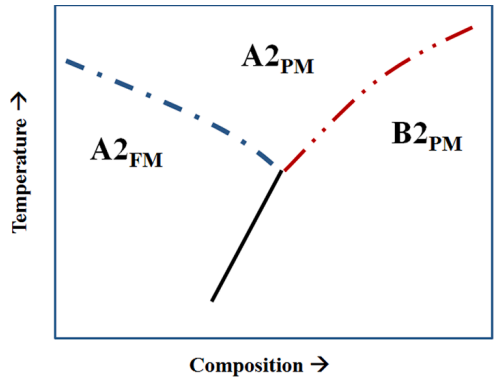

Fig. 20. A constant pressure Temperature/Composition schematic phase diagram which displays an incorrect representation of phase equilibria in a system exhibiting intersecting higher order transitions.

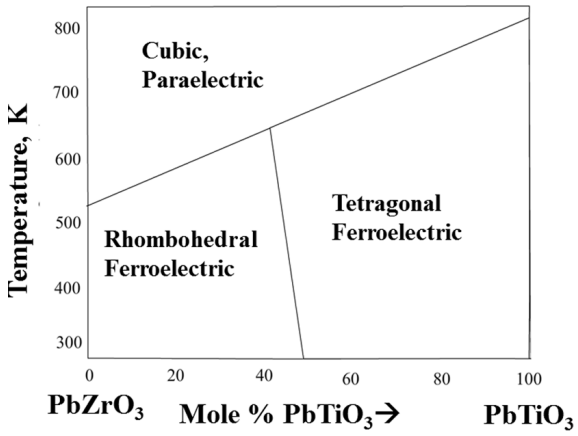

Fig. 21. A schematic constant pressure Temperature/Composition phase diagram of the $PbZrO_3/PbTiO_3$ binary system which often appears in the literature in this form. The nearly vertical line is called a morphotropic phase boundary. Construction errors exist in the diagram and are discussed in the text.

3.5.4.2. Tetracritical points. A Temperature/Composition phase diagram with a *Tetracritical* point is depicted in Fig. 19 Below the intersection of the two higher order transitions lines (the tetracritical point) there is a one phase field, namely, that of the ferromagnetically ordered B2 atomically ordered phase (CsCl). This phase has two order parameters, one for the magnetic ordering and the other from the atomic ordering transition.

For this diagram there are four higher order transitions:

$A2_{PM} \rightarrow A2_{FM}$
$A2_{FM} \rightarrow B2_{FM}$
$A2_{PM} \rightarrow B2_{PM}$
$B2_{PM} \rightarrow B2_{FM}$

All phase boundaries are lines separating single phase fields in this diagram which is not a violation of the Gibbs Equilibrium Phase Rule, since the transformations are higher order. Included on the diagram are the extensions of the higher order transition lines through the tetracritical point. These are helpful in determining the transformation paths of alloys that are quenched from the high temperature disordered phase and therefore proceed at temperatures that are far from equilibrium. See [27] for a detailed discussion of transformation paths.

3.5.5. Higher order transition curves exhibiting construction errors

The Temperature/Composition phase diagram shown in Fig. 20 is an example of an incorrect construction in a diagram that contains two intersecting higher order transition curves. The first order solid line which appears to display a two phase equilibrium between the $A2_{FM}$ and $B2_{PM}$ phases cannot be represented by a solid line, but should be a two phase field as shown in Fig. 18 for the bicritical diagram. Two single phase regions must have a two phase region between them for Gibbsian first order transformations. Indeed as incorrectly displayed in Fig. 20, the two phases portrayed to be in equilibrium along the solid boundary have the same composition which can only occur at maxima or minima in first order phase diagrams. See Section 3.1.2 above.

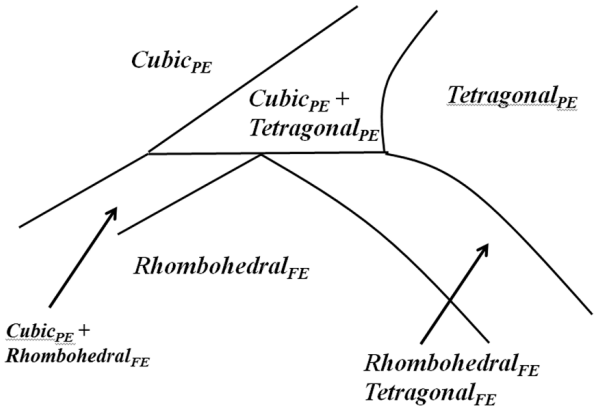

Fig. 22. A possible correction to phase diagram shown in Fig. 21 in the area near the three phase region. This alternative diagram was suggested by [29] and displays a peritectoid three phase equilibrium in conformity with the Gibbs Equilibrium Phase Rule for first order phase transformations.

A schematic phase diagram of the $PbZrO_3/PbTiO_3$ binary phase diagram (PZT) is shown in Fig. 21. The three phases shown are the cubic high temperature, paraelectric Perovskite phase, the tetragonally distorted Perovskite ferroelectric phase and the rhombohedrally distorted Perovskite ferroelectric phase. The transitions between both the cubic and tetragonal phase and the cubic to rhombohedral phase are first order as determined by the Landau symmetry rules [28]. So is the tetragonal to rhombohedral transition across what is called the morphotropic phase boundary. Also, from Polarization vs. temperature plots the diagrams are known to be first order but weakly so. Such diagrams have been discussed by Khachaturyan and co-workers [29]. It is clear that this diagram as drawn in Fig. 21 violates the Gibbs Phase Rule for first order transitions since there should be two phase regions between the single phase regions. Also the diagram depicts three phases in equilibrium at one composition, temperature and pressure, another violation of the Gibbs Phase Rule. Fig. 22 shows one way that [29] suggest to reconfigure the diagram to have it conform with the Gibbs Equilibrium Phase Rule. It should be noted that Fig. 22 is a greatly expanded near the "three phase point" of Fig. 21. Such a diagram shows that what has been termed a "morphotropic phase boundary" is really the lower section of a possible peritectoid transformation and consists of two phase regions on either side of the rhombohedral ferroelectric phase. This interesting region should give rise to interesting microstructures which depend on the processing variables and therefore will also give rise to interesting ferroelectric properties.

Another problem with the diagram displayed in Fig. 21 is that it shows single phase regions of varying compositions at low temperatures. This points to a violation of the Third Law of Thermodynamics. More work must be performed on the equilibrium configuration of the phase diagram in this well studied and utilized material.

4. Concluding remarks

Equilibrium Phase Diagrams of alloys are important tools for the Materials Scientist in understanding the behavior of the alloys during processing and susequent application. It is important that the diagrams published in the literature be correct in their details as subtle differences in them can bring in large differences in expected behavior of the materials systems. In this paper we have reviewed some of the construction errors which are found in unary and binary diagrams and have categorized them as:

1. Departures from the Gibbs Equilibrium Phase Rule
2. Incorrect Phase Boundary Configurations
3. Thermodynamically Improbable Aspects of some Phase Diagrams
4. Errors related to the Third Law of Thermodynamic
5. Incorrect constructions of Higher Order Phase Transitions

Multi-component phase diagrams are of course subject to similar possible errors as those discussed in this review. In addition, we are aware that the majority of alloys utilized in applications are likely to be far from being in true thermodynamic equilibrium. Thus care must be made in the application of the principles discussed in this paper.

More and more diagrams are being published that are based on computer modeling and it is hoped that this paper will steer authors of such works to be alert for constructions which may be in violation of thermodynamic principles. Indeed, perhaps the computers can "learn" to look out for such construction errors by the process of "machine learning".

Declaration of Competing Interest

The authors declare that they have no known competing financial interests or personal relationships that could have appeared to influence the work reported in this paper.

Acknowledgments

DEL acknowledges the financial support of the ALCOA chair of Physical Metallurgy at Carnegie Mellon University as well as partial support from the National Science Foundation, Grant DMR-1709247. TBM acknowledges his long term work with Dr. H. Okamoto on "improbable Phase Diagrams". Both authors express their thanks for many conversations on phase equilibria with their friend and colleague Professor William A. Soffa of the University of Virginia.

Appendix A. Impossible phase diagram constructions

A phase diagram with multiple errors of construction taken from Okamoto and Massalski [20] is included here because of its relevance to the present paper. Brief discussions of the types of errors are included.

A: The melting temperature of a single component is the same temperature as its solidification temperature. This follows from the reduced Gibbs Equilibrium Phase rule for one component system at fixed pressure, in which the number of components is $C = 1$, the number of phases, $\Phi = 2$ (the liquid and the solid) and thus, the degree of freedom $\mathscr{F} = 0$, Since there is no degree of freedom, the liquidus and solididus must meet at one temperature on the %B = 0 axis.
B. When two liquidus curves meet, three phases are in equilibrium. Thus by the reduced Phase rule the degree of freedom, $\mathscr{F} = 0$, and the curves must both meet at the eutectic point on the temperature invariant line of the three phase equilibrium.
C. A tie line must terminate at a phase boundary.
D. The solvus curve of the α phase in equilibrium with the ε phase, must be of the same composition as the solvus curve of the α phase in equilibrium with δ phase, since they must meet at one point of the three phase invariant temperature (peritectoid) line.
E. A phase boundary must extrapolate into a two-phase field after crossing an invariant point. This is discussed above in Section 3.1 and displayed in Fig. 6.
F. One phase boundary of a two phase field can not intersect the 0% vertical axis except at 0 K. There must be some solubility of B in A at all temperatures above 0 K, by the second law of thermodynamics.
G. The top of the γ phase boundary must intersect and end at the invariant peritectic reaction line.
H. In binary equilibrium phase diagrams an invariant line must display equilibrium among three phases, since for two-components, $F = 0$ only when the number of phases is three. The horizontal line should be removed.
I There must be a two phase region between two single phase regions (δ and ε) in binary phase diagrams, displaying first order phase transformations.
J. When two single phase regions meet within a binary phase diagram they must do so at a minimum or at a maximum.
K. The slopes of the temperature composition curves at congruent points must be zero. See Section 3.1.2.
L. A local minimum in a single-phase field cannot be drawn without an additional boundary in contact with it. This minimum would display two fixed compositions of the same phase at a temperature just above the minimum, violating the Gibbs Equilibrium Phase Rule.
M. A local maximum in a single-phase field cannot be drawn without an additional boundary in contact with it. Just below the maximum at a fixed temperature two phases would be in equilibrium with no degree of freedom, violating the Gibbs Equilibrium Phase Rule.
N. The line must be horizontal since it displays three phases to be in equilibrium with each other, which can only happen when the temperature is fixed in a binary phase diagram.
O. A phase boundary cannot terminate within a phase field.
P. Similar to case K above: in this case it is both the liquid and the solid which do not have zero slopes of the temperature composition curves. See discussion in Section 3.1.2.
Q. The point at Q displays the end point of a three phase equilibrium with two of the phases having the same composition. There are too many constraints in this configuration, (3 phases means $\mathscr{F} = 0$, and the compositions of β_1 and the liquid are equal, adding a 4th constraint, which would yield an impossible negative degree of freedom for the system!)
R. The initial slopes of the liquidus and solidus must have the same sign. See discussion on the slopes of the temperature composition curves at near melting point (the van't Hoff relation) in Section 3.3.2.
S. The horizontal line displays four phases to be in equilibrium, which is impossible in a binary phase diagram of a system of constant pressure.
T. Two separate phase boundaries of two-phase fields can not cross one another. At the point of intersection, the composition of the two phases would be the same, as would be their temperature, in violation of the Gibbs Equilibrium Phase Rule.
U. Since the abscissa of this diagram is at T = 0 K, the solubility of A in β_2 should be 0, according to the third law of thermodynamics. Also, the solubility of the five intermetallic compounds should be zero at 0 K, according to the Third Law of Thermodynamics.

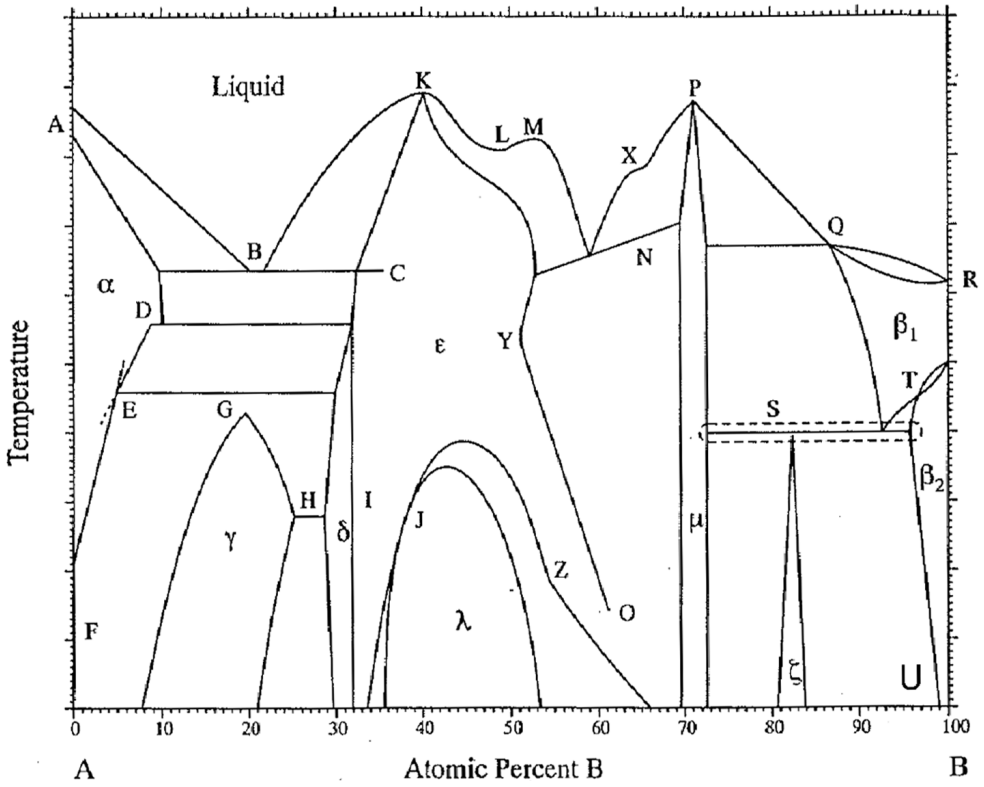

Fig. A.1. A binary phase diagram displaying multiple errors of construction. The pressure is assumed to be constant. All phase transformations are assumed to be thermodynamically first order [see 20]. The abscissa corresponds to T = 0 K.

Appendix B. Improbable phase diagram constructions

The phase diagram and some of the discussions in this appendix derive from those first presented in Okamoto and Massalski [20] and are included here because of their relevance to the present paper.

a. The initial opening angle of the Vapor (V) + L two-phase field at 0 at.% B should be much greater than that of the L + S two-phase field because the heat of vaporization of an element is much greater than its heat of fusion. This can be seen from the van't Hoff relation discussed in Section 3.3.2
b. The extrapolation of the L/L + γ liquidus crosses the 0 at.% line (problem F in the Fig. A.1 of Appendix A) in the metastable state. The liquidus cannot be extrapolated below 0 at.% even in the metastable state. If an attempt is made to avoid this problem in this case, the liquidus must be curved sharply in the metastable region.
c. The slope of the liquidus curve is too flat compared to those at point *e*. The entropies of fusion of most elements are similar (Richard's law), and the trend is the same for intermediate phases. When multiple intermediate phases exist in a system, the sharpness of the liquidus curves should be similar. This is also applicable to extrema in metastable regions (see Fig. B.1).
d. The liquidus of the γ phase which becomes unstable at low temperatures (shown as *d*) must have a larger curvature at the melting point. The entropy of fusion of a phase that is unstable at low temperatures is small, and the liquidus would be more pointed as a result.
e. Opposite to the case of *c*. The liquidus at *e* is too sharp in comparison with the liquidus at *c*.
f. When the L/L + λ liquidus is extrapolated, the peak should appear at around the composition of λ. A rapid change of curvature would be required near the peak, and the peak would be extremely pointed also.
g. The congruent melting point of the A_mB_n compound is too far from its stoichiometric composition.
h. Two phases (δ and λ) with similar compositions are unlikely to coexist in stable forms over a wide temperature range.
i. In the metastable state, ε is shown to transform into A_mB_n. A stoichiometric phase is unlikely to do this.
j. The transformation temperature of ε to β_2 should be higher than the melting temperature of ε. Otherwise the β_2 phase would be stable above *j*.
k. Extrapolation of the two boundaries of L and β_2 should not cross. See problem T in Appendix A.
l. The transformation at the peritectoid point should not be zero slope.
m. The β_2/σ solvus cannot have zero slope when it ends at the peritectoid temperature.
n. The liquid miscibility gap is too close to the 100% B axis. Such a miscibility gap can form only when an unnatural thermodynamic model is used.

o. The slope is too steep
p. The liquidus and solidus of the β_3 phase must cross on the 100 at.% B line at the metastable melting temperature of β_3
q. The two phase boundaries should have different initial slopes.
r. The slopes of the β_1 and β_2 boundaries are too different for an allotropic transformation.

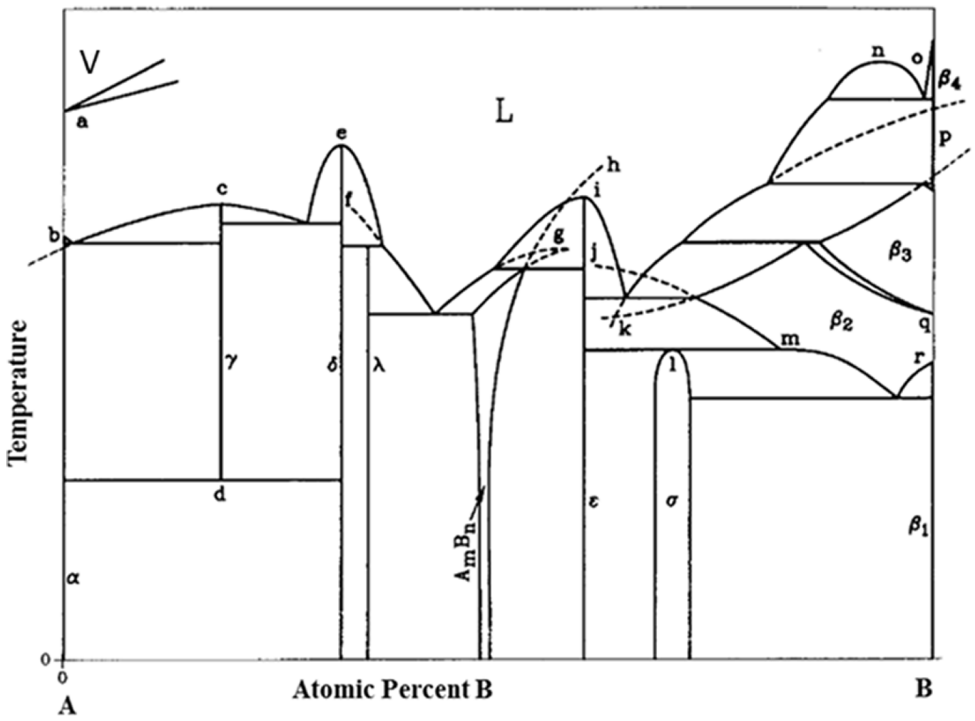

Fig. B.1. A Temperature/Composition binary phase diagram displaying multiple improbable constructions. The pressure is assumed to be constant. All phase transformations are assumed to be thermodynamically first order [see 20]. The abscissa corresponds to T = 0 K.

References

[1] Soffa WA, Laughlin DE. Diffusional phase transformations in the solid state. In: Laughlin David E, Hono Kazuhiro, editors. Physical Metallurgy. three volumes (5th ed.). Elsevier; 2014. p. 851–1029.
[2] Gaskell DR, Laughlin DE. Introduction to the thermodynamics of materials. 6th ed. Taylor-Francis; 2017.
[3] Morey GW. The phase rules and heterogeneous equilibrium. In: Commentary on the Scientific Writings of J. Willard Gibbs. Yale University Press; 1936.
[4] Findaly A. The phase rule and its applications, 9th ed. revised by Campbell AN, Smith NG. Dover Publications; 1951.
[5] Ricci JE. The phase rule and heterogeneous equilibrium. D. Van Nostrand and Company; 1951.
[6] Zernike J. Chemical phase theory. A comprehensive treatise on the deduction, the applications and the limitations of the phase rule. Klewer; 1955.
[7] Dehoff R. Thermodyanmics in materials science. 2nd ed. Taylor and Francis; 2006.
[8] Rhines FN. Phase diagrams in metallurgy: their development and application. New York: McGraw-Hill Book Co. Inc; 1956.
[9] Prince A. Alloy phase equilibria. Amsterdam, Netherlands: Elsevier Publishing Co.; 1966.
[10] Gordon P. Principles of phase diagrams in materials systems. New York: McGraw-Hill Book Co.; 1968.
[11] Zen E-An. Construction of pressure-temperature diagrams for multicomponent systems after the method of Schreinemakers – a geometric approach. U.S. Geol. Surv. Bull. 1225; 1984.
[12] Andrews T. The Bakerian lecture: on the gaseous state of matter. Phil. Trans. Roy. Soc 1869;159:575–90.
[13] van der Waals JD. Over de continuiteit van den gas- en vloeistoftoestand. (On the Continuity of the Gaseous and Liquid States), Universiteit Leiden; 1873.
[14] Ehrenfest P. Phasenumwandlungen im ueblichen und erweiterten Sinn, classifiziert nach dem entsprechenden Singularitaeten des thermodynamischen Potentiales. Verhandlingen der Koninklijke Akademie van Wetenschappen. Amsterdam 1933;36:153–57.
[15] Laughlin DE. The beta iron controversy revisited. J Phase Equilib Diffusion 2018;39:274–9. https://doi.org/10.1007/s11669-018-0638-z.
[16] Laughlin DE. Magnetic transformations and phase diagrams. Metall Mater Trans 2019;50A:2555–79.
[17] Wagner C. Thermodynamics of alloys. Cambridge Mass.: Addison Wesley Press; 1952.
[18] Goodman DA, Cahn JW, Bennett LH. The centennial of the Gibbs-Konovalov rule for congruent points. Bull Alloy Phase Diagrams 1981;2(1):29–34.
[19] Massalski TB, editor. Binary alloy phase diagrams. 2nd ed. Materials Park (OH): ASM International; 1990.
[20] Okamoto H, Massalski TB. Thermodynamically improbable phase diagrams. J Phase Equilib 1991;12(2):148–68, and Thermodynamically Improbable Phase Diagrams, Science and Dynamics of Alloy Phase Trasformations, Turchi, PEA and Gonis, A, editors, Plenum press; 1994.
[21] Lupis CHP. Chemical thermodynamics of materials. Elsevier; 1983.
[22] Gaye H, Lupis CHP. Numerical techniques in the calculation of binary diagrams. Metall Trans 1975;6A(5):1049–56.
[23] Laughlin DE, Soffa WA. The third law of thermodynamics: phase equilibria and phase diagrams at low temperatures. Acta Mater 2018;145:49–61.
[24] Abriata JP, Laughlin DE. The third law of thermodynamics and low temperature phase stability. Prog Mater Sci 2004;48(3):367–87.
[25] Federov PP. Third law of thermodynamics applied to phase diagrams. Russ J Inorg Chem 2010;55(11):1722–39.
[26] Meijering JL. Miscibility gaps in ferromagnetic alloy systems. Philips Res Rept 1963;18:318–30.

[27] Laughlin DE, Soffa WA. Exsolution, ordering and structural transformations: systematics and synergistics. Physical properties and thermodynamic behaviour of minerals; 1987. p. 213–64.
[28] Landau LD, Lifshitz EM. Statistical physics. 3rd ed. Oxford: Pergamon; 1980.
[29] Rossetti GA, Zhang W, Khachaturyan A. Phase coexistence near the morphotropic phase boundary in lead zirconate titnate solid solutions. Appl Phys Lett 2005; 88:072912.